Journal of Materials Chemistry B

Accepted Manuscript

ROYAL SOCIETY OF CHEMISTRY

www.rsc.org/materialsB

Journal Name

RSCPublishing

ARTICLE

A Recyclable Carbon Nanoparticles-Based Fluorescent Probe for Highly Selective and Sensitive Detection of Mercapto Biomolecules

?Cite this: DOI: 10.1039/x0xx00000x

Received 00th January 2012,
Accepted 00th January 2012

DOI: 10.1039/x0xx00000x

www.rsc.org/

Minhuan Lan, [a] Jinfeng Zhang, [a] Ying-San Chui, [a] Hui Wang, [b] Qingdan Yang, [a] Xiaoyue Zhu, [a] Huaixin Wei, [a] Weimin Liu, [b] Jiechao Ge, [b] Pengfei Wang,* [b] Xianfeng Chen, [a] Chun-Sing Lee, [a] and Wenjun Zhang* [a]

Carbon nanoparticles (CNPs) with strong blue emission are synthesized using a microwave-assisted hydrothermal method. The fluorescence of the CNPs can be completely quenched by Hg^{2+} through effective electron or energy transfer process due to synergetic strong electrostatic interaction and metal-ligand coordination. Based on this, a system containing Hg^{2+}-quenched CNPs (CNPs-Hg^{2+}) is designed to be a sensitive and selective turn-on fluorescent probe towards cysteine (a type of mercapto biomolecules) with a detection limit of 15 nM. The fluorescence of CNPs-Hg^{2+} aqueous solution can be repeatedly turned on and off for over 10 times by alternative addition of cysteine and Hg^{2+}, respectively. After 10 cycles, the fluorescence intensity could be recovered to as high as 85% of the original value of CNPs. Remarkably, the sensing process is able to be observed by naked eyes under UV irradiation. Furthermore, the sensing is specific to biothiols and the sensor is able to work in living cells.

Introduction

Mercapto biomolecules including cysteine (Cys), homocysteine (Hcy), and glutathione (GSH) play a crucial role in cellular antioxidant defense systems, and in maintaining biological redox homeostasis through the equilibrium established between reduced free thiols (RSH) and oxidized disulfides (RSSR).[1-3] An abnormal level of thiols in biological system can be regarded as an indicator of health issues such as liver damage, skin lesions, cardiovascular diseases, and cancers.[4-7] The specific and sensitive determination of mercapto biomolecules is thus of particular interest in biological and toxicological diagnosis.

Conventional analytical assays like mass spectrometry, gas chromatography, high-performances liquid chromatography and electrochemical methods generally require expensive instruments and/or sophisticated sample preparation. These issues stimulate the development of new techniques for sensing thiols.[8-11]

Recently, fluorescent sensors for detecting biomolecules have attracted increasing attention due to their superiority in virtue of their high sensitivity, simplicity, rapid response, and the capability to be applied in both solution and solid phases.[12-16] Various organic dyes and semiconductor quantum dots probes have been reported for detecting mercapto biomolecles.[17-20] However, their problems on water solubility, photostability, and/or pH-stability still need to be resolved for practical applications. Moreover, few organic dye-based sensors display fluorescent reversibility which is essential for real-time monitoring of the dynamic biological processes in living cells.[21-22] To achieve a desirable technology for sensing mercapto biomolecules with combined superior advantages, a variety of materials is currently being actively developed. Among the efforts, the recent discovery of photoluminescence effect of carbon nanoparticles (CNPs) has attracted increasing research interest.[23] Comparing to traditional semiconductor quantum dots and organic polymer dots, these carbon nanomaterials are featured with a number of strengths covering outstanding chemical inertness, excellent photo-stability, favourable biocompatibility, and good water solubility.[24-37] As an excellent fluorescence material, through surface functionalization and/or combination with other nanomaterials, CNPs have been used as probes for sensing various metal ions and biomolecules including proteins.[38-44] For example, Shi et al. reported a dual-mode nanosensor with both colorimetric and fluorometric readout based on integration of CNPs and gold nanoparticles for detection of GSH in distilled water.[45] However, the fluorescence intensity increased only by ~25% upon addition of 3 μM of GSH and a long response time of ~5 min was needed. Moreover, the influence of pH values on the sensing characteristics and the reversibility of the probes were not presented. Table S1 summarizes the sensing performance of some recently-reported fluorescence thiols sensors based on

CNPs. It can be noted that the response time, pH stability, PL recovering efficiency, and recyclability need to be further improved for practical applications.

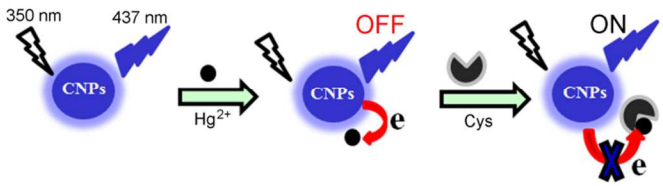

Scheme 1. Schematic diagram showing the fabricating process of the CNPs-Hg^{2+} sensor. The fluorescence of the sensor can be turned on by addition of Cys.

In this work, water-soluble CNPs with a fluorescence quantum yield of about 0.3 are prepared by a simple microwave-assist hydrothermal method using melamine and trisodium citrate dihydrate as precursors. As shown in Scheme 1, we purposely quench the strong blue emission of CNPs and use the integrated system of Hg^{2+}-quenched CNPs (CNPs-Hg^{2+}) as a non-fluorescent sensor. This sensor can be conveniently employed as a fluorescence turn-on sensor for sensitive detection of mercapto biomolecules such as Cys, Hcy and GSH. Attractively, the sensor is able to be regenerated by further addition of Hg^{2+} and reused for over 10 times. Furthermore, such a CNPs-Hg^{2+} system is capable of imaging mercapto biomolecules in living cells.

Experimental

Materials

Melamine, trisodium citrate dihydrate, N-Ethylmaleimide (NEM), NaCl, KCl, $Mn(OAc)_2$-$4H_2O$, $Co(OAc)_2$, $Ni(OAc)_2$, $Al(NO_3)_3$-$9H_2O$, $Cu(OAc)_2$-H_2O, $FeCl_3$, $Cs(OAc)_2$-H_2O, $CeCl_3$-$7H_2O$, $LiNO_3$, $Ba(OAc)_2$, $MgCl_2$-$6H_2O$, $CdSO_4$, $HgCl_2$, HEPES, RNA, DNA, Cysteine (Cys), Homocysteine (Hcy), Glutathione (GSH), Serine (Ser), Valine (Val), Tyrosine (Tyr), Leucine (Leu), Tryptophan (Trp), Alanine (Ala), Aspartic acid (Asp), Methionine (Met), Threonine (Thr), Isoleucine (Ile), Glycine (Gly), Argine (Arg), Lysine (Lys), and 3-(4,5-dimethylthiazol-2-yl)-2,5-diphenyltetrazolium bromide (MTT) were purchased from Sigma-Aldrich Co. LLC. All chemicals were used as received without further purification. Deionized water with a conductivity of 18.2 MΩ cm^{-1} was purified through a Millipore water purification system.

Characterizations

The absorption spectra were recorded on a Shimadzu 1700 spectrophotometer using 10 mm path length quartz cuvettes in the range 250-600 nm, while the fluorescence measurements were carried on a Horiba Fluormax-4 spectrophotometer at room temperature. X-ray photoelectron spectroscopy (XPS) analysis was measured on a VG ESCALAB 220i-XL surface analysis system. X-ray diffraction (XRD) pattern was obtained using an X-ray diffractometer (Bruker, D2 PHASER). Fourier transform infrared spectroscopy (FTIR) was performed on an IFS 66 V/S (Bruker) IR spectrometer in the range of 400-4000 cm^{-1}. Transmission electron microscopy (TEM) was performed on a Philips CM200 electron microscope. Fluorescence quantum yield was determined according to an established procedure with quinine sulfate in 0.1 M H_2SO_4 as a standard (54%). All pHs were measured with a Eutech pH-meter PH 700.

Preparation of fluorescent CNPs

CNPs were prepared by microwave-assisted hydrothermal treatment of melamine and trisodium citrate dihydrate. In a typical synthesis, 0.12 g of melamine and 0.58 g of trisodium citrate dihydrate were added into 25 mL of H_2O. Then the mixture solution was transferred into a microwave reactor and maintained at 180 °C for 12 hours. After cooling to room temperature, the CNPs were collected by removing the large particles though filtering using 0.22 μm membranes, and dialyzed using distilled water for two days. CNPs aqueous solution was stored at 4 °C for future characterization and use.

Sensor preparation and its application for sensing Cys

10 μM of Hg^{2+} was added to 4 μg/mL of the as-synthesised CNPs to make a sensor (CNPs-Hg^{2+}). This integrated sensor does not possess fluorescence and was used for sensing Cys. In a typical run, 40 μL of CNPs dispersion solution (0.2 mg/mL) was added into 2 mL HEPES buffer solution (10 mM, pH 7.2), and then 10 μL of Hg^{2+} (2 mM) was added to the CNPs solution, followed by the addition of calculated amount of Cys. The sensitivity and selectivity measurements were conducted in triplicate. After the test, the sensor was regenerated by adding 10 μM of Hg^{2+} ions.

Cell culture and *in vitro* imaging studies

A549 cells were obtained from the Peking Union Medical College and cultured in culture media (DMEM/F12 supplemented with 10% FBS, 50 unit/mL penicillin, and 50 μg/mL of streptomycin) at 37 °C in a humidified incubator containing 5% CO_2. For cell imaging studies, cells were seeded in a 6-well plate at a density of 10^4 cells per well in culture media and maintained at 37 °C in a 5% CO_2/95% air incubator for 24 hours. A549 cells were pretreated with 4 mM NEM for 1 hour to reduce the concentration of thiol-containing biomolecules, and then they were incubated with 100 μL of CNPs aqueous solution in culture media for another 4 hours at 37 °C. After the medium was removed and the cells were carefully washed with PBS twice, the cells were then incubated with 20 μM Hg^{2+} aqueous solution for another 5 minutes at 37 °C. Fluorescence imaging of living A549 cells was performed under Nikon fluorescence microscopy (excitation light source: 330-380 nm). Lastly, the cells treated with NEM, CNPs and Hg^{2+} were incubated with 50 μM Cys aqueous solution for another 5 minutes at 37 °C, and imaged using fluorescence microscopy. Confocal laser scanning microscopy images of A549 cells incubated with CNPs were obtained using Leica SPE confocal laser scanning microscope with a 405 nm laser.

MTT assay

A549 cells were seeded in a 6-well plate at a density of 10^4 cells per well in culture media and maintained at 37 °C in a 5% CO_2/95% air incubator for 24 hours. Then, the culture media was removed and the cells were incubated in culture medium containing as-prepared CNPs with different concentrations (0~500 μg/mL) for 24 hours in the presence of 10 μM Hg^{2+} and washed with the culture medium. An amount of 200 μL of the new culture medium (without FBS) containing MTT (20 μL, 5 mg/mL) was then added, followed by incubating for 4 hours to allow the formation of formazan crystals. Absorbance was measure at 570 nm. Cell viability values were determined according to the following formulae: Cell viability (%) = the absorbance of experimental group/the absorbance of control group × 100%.

Results and discussion

Structure and Composition of CNPs

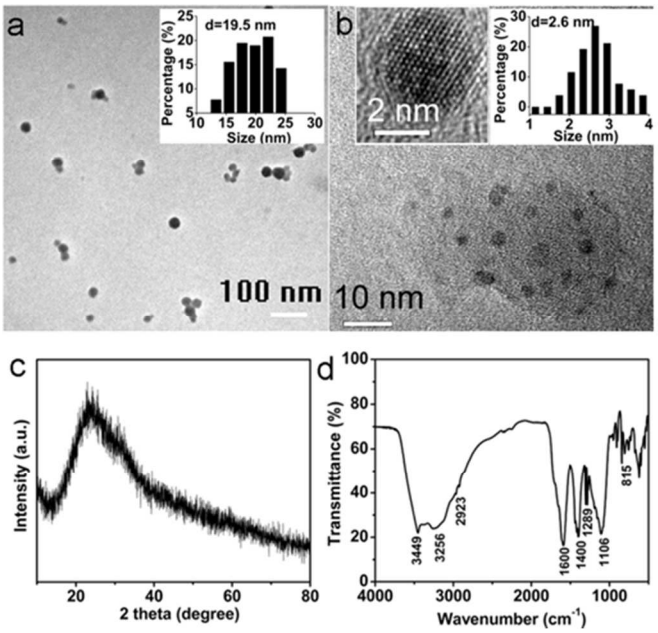

Fig. 1. (a) and (b) TEM images of CNPs. The insets show the particle size distribution histograms (n=50) and HRTEM image of CNPs. (c) The XRD pattern and (d) FTIR spectrum of the CNPs.

Fig. 1a shows a TEM image of CNPs. The inset histogram reveals a size distribution of nanoparticles around 19.5 nm. High-resolution TEM (HRTEM) observation in Fig. 1b further shows that a nanoparticle is composed of several crystalline carbon quantum dots (left inset in Fig. 1b) embedded in an amorphous matrix. The right inset depicts a diameter distribution of quantum dots around 2.6 nm. Fig. 1c is a typical XRD pattern which presents only one broader peak at 2θ=24°. This is consistent with the result shown in previous reports of CNPs.[46, 47] The Fourier transform infrared (FTIR) spectrum was acquired to determine the surface functional groups of the CNPs and the result is in Fig. 1d. The peak at 3449 cm^{-1} is ascribed to the characteristic absorption band of N-H stretching vibration mode and the peaks at 3256 and 1106 cm^{-1} are attributed to the stretching vibration of -OH. The peaks at 1600 and 1400 cm^{-1} indicate the existence of COO^-. The characteristic absorption band of C-OH stretching vibration at 1289 cm^{-1} is also observed, and the peaks at 2923 and 815 cm^{-1} can be assigned to the C-H stretching vibration mode and C-H out-of-plane bending mode.

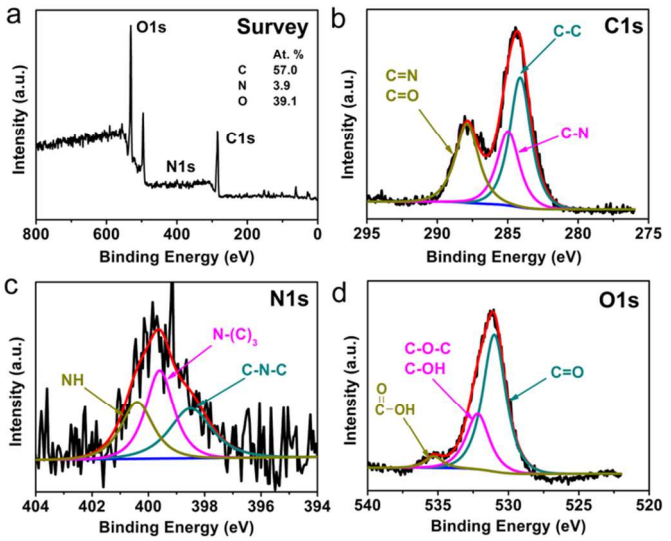

Fig. 2. (a) XPS survey spectrum, and (b) C1s, (c) N1s and (d) O1s high-resolution spectra of the CNPs.

The surface composition and elemental analysis for the CNPs were further characterized by X-ray photoelectron spectroscopy (XPS). Three peaks at about 284.5, 399.5 and 531.5 eV are presented in the XPS survey spectrum of CNPs (Fig. 2a) and correspond to C1s, N1s and O1s core levels, respectively. The C/N/O atom ratio was calculated to be 57.0/3.9/39.1. The high-resolution XPS spectrum of C1s (Fig. 2b) can be resolved into three peaks with binding energies of about 284.2, 285.0 and 287.9 eV, corresponding to C-C, C-N and C=N/C=O, respectively. Deconvolution of the N1s spectrum in Fig. 2c shows three peaks at 398.5, 399.6 and 400.4 eV for C-N-C, N-$(C)_3$ and N-H bonds, respectively. The fitting of the O1s peak gives three components at 531.0, 532.2 and 535.3 eV for C=O, C-OH/C-O-C and COOH groups, respectively (Fig. 2d). The XPS analysis agrees well with that of the above FTIR observations. These findings suggest that the surfaces of the CNPs be functionalized with amino, hydroxyl and carboxylic/carbonyl moieties originated from melamine and trisodium citrate dihydrate.

The zeta-potential of the CNPs aqueous solution was measured to be -56.7 mV (Fig. S1).

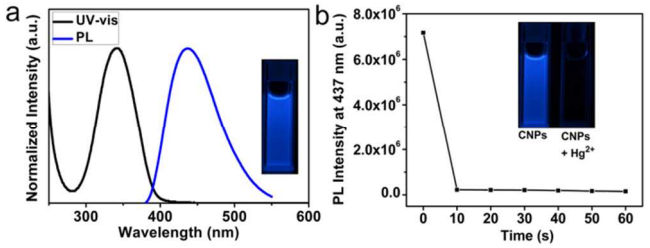

Fig. 3. (a) Normalized UV-vis absorption (black line) and PL (blue line) spectra of the CNPs in aqueous solution (λ_{ex}=350 nm). Inset: the photograph of CNPs solution under a UV light (365 nm). (b) The variation of PL intensity of CNPs at 437 nm upon addition of 10 μM of Hg^{2+} in HEPES buffer solution; the observation time interval is 10 s. The inset shows the photograph of CNPs solutions in the absence and presence of 10 μM Hg^{2+} under UV light.

Fig. 3a presents the normalized UV-Vis absorption and PL spectra of CNPs dispersed in aqueous solution. It reveals that CNPs have an absorption peaked at 342 nm and a blue emission peaked at 437 nm when excited at 350 nm. No obvious wavelength shift is observed in the PL spectra of CNPs as the excitation wavelength varies (Fig. S2). In line with the PL measurement, the CNPs aqueous solution under a UV light (365 nm) exhibits a strong blue fluorescence (Fig. 3a, inset) with a fluorescence quantum yield of 0.3 using quinine sulfate as a reference.[48-50] Attractively, the PL intensity of these CNPs can be maintained even at high ionic strength conditions (1 mol/L NaCl solution, Fig. S3) or after irradiation for 1 hour by 350 nm xenon lamp equipped in the FL spectrometer (Fig. S4). Analysis of the fluorescence decay kinetics at 437 nm revealed a single exponential decay with a lifetime of 7.0 ns (Fig. S5), suggesting the singlet state nature of the emission.

CNPs-Hg^{2+} for sensing biothiols as a fluorescence turn-on sensor

The strong blue emission of CNPs solution can be completely quenched in 10 seconds upon addition of 10 μM Hg^{2+} solution, as shown in Fig. 3b and Fig. S6. The quenching is able to be directly observed by naked eyes under a UV light (Fig. 3b, inset). Prolonging the reaction time does not lead to further reduction of PL intensity. The fluorescence quenching of CNPs by Hg^{2+} has been elucidated to be presumably due to nonradiative electron/hole annihilation through effective electron or energy transfer process resulted from strong electrostatic interaction and metal-ligand coordination between CNPs and Hg^{2+}.[38, 44]

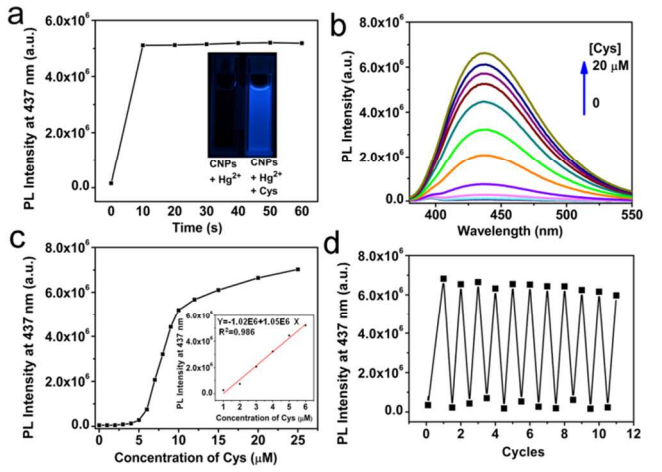

Fig. 4. (a) The variation of PL intensity of CNPs-Hg^{2+} at 437 nm upon addition of 10 μM of Cys in HEPES buffer solution; the observation time interval is 10 s. The inset shows the photograph of the solution in the absence and presence of Cys under UV light. (b) Dependence of PL spectra of CNPs-Hg^{2+} in HEPES buffer solution (10 mM, pH 7.2) on the gradual addition of Cys from 0 to 20 μM. (λ_{ex}=350 nm). (c) Dependence of PL intensity at 437 nm with incremental addition of Cys. Insert: PL intensity of CNPs-Hg^{2+} solution at 437 nm versus the concentrations of Cys, the measurements were performed using CNPs-Hg^{2+} solution with 4 μM Cys pre-added as the. (d) The PL intensity at 437 nm of CNPs-Hg^{2+} in HEPES buffer solution upon alternative addition of 20 μM of Cys and 10 μM of Hg^{2+}. The concentrations of Hg^{2+} and Cys in the last cycle were 0.5 mM and 1.0 mM, respectively.

In this non-fluorescent CNPs-Hg^{2+} system, if we add mercapto biomolecules including Cys, Hcy, and GSH, the fluorescence can be dramatically increased due to a previously described competition mechanism.[51, 52] The time-dependent fluorescence spectra of the CNPs-Hg^{2+} against 10 μM Cys in HEPES buffer solution (10 mM, pH 7.2) was collected at room temperature. The spectra are shown in Fig. S7 and the fluorescence intensities at different times are in Fig. 4a. Obviously, the PL intensity of CNPs-Hg^{2+} aqueous solution dramatically increases within 10 seconds upon addition of 10 μM Cys. These results verified that the CNPs-Hg^{2+} system can function as a fluorescence turn-on sensor with fast response for biothiols. The thiol groups as strong Hg^{2+} chelators are able to remove Hg^{2+} from CNP surfaces through the formation of Hg-S bonds.

The effects of the synthetic parameters of CNPs including the molar ratio of precursors, reaction time and reaction temperature on their sensing properties were studied, as summarized in Table S2. It can be seen that the CNPs prepared under different conditions show similar UV-vis spectra (Fig. S8), and their PL emission peaks have no obvious shift under excitation for wavelengths varying from 300 nm to 400 nm. A maximum PL intensity at about 437 nm was observed for all samples under the excitation at 350 nm. Furthermore, the fluorescence quantum yields (QY) of all CNPs were calculated to be around 0.3 with excitation at different wavelengths. For all samples, their PL emissions could be quenched by Hg^{2+} and then recovered by Cys, as shown in Fig. S9(A-G). However, the PL quenching efficiency and recovering efficiency were different for the samples prepared under different reaction

conditions. The CNPs prepared using the conditions described in the Experimental (denoted as CNPs-D in Table S2) showed the best overall performance and was therefore used as the sensing platform in this work.

Absorption and fluorescence titration experiments were carried out to illustrate the spectra response of our CNPs-Hg^{2+} system to Cys of different concentrations. As shown in Fig. S10a, the absorption peak of CNPs-Hg^{2+} at 318 nm red-shifts to 335 nm in the presence of Cys. Considering that there is no obvious absorbance of Hg^{2+}, Cys and Hg^{2+}-Cys solutions in the wavelength range of from 300 to 400 nm (Fig. S10b), the observed red-shift should be attributed to the interactions between Cys with Hg^{2+} and groups (such as amino, hydroxyl and carboxylic/carbonyl) on the CNP surfaces. The dependence of the PL of CNPs-Hg^{2+} on the concentration of Cys is shown in Fig. 4b and 4c. The increase of the concentration of Cys from 0 to 4 μM only slightly changes the PL intensity. However, further addition of Cys leads to a sharp increase of PL intensity. Based on these results, it is ideal to prepare a CNPs-Hg^{2+} solution containing 4 μM Cys for sensor applications. To demonstrate this, the dependence of PL intensity of the CNPs-Hg^{2+} solution with 4 μM Cys at 437 nm on the concentrations of further added Cys is presented in the inset of Fig. 4c, inset. A good linear relationship between the added Cys and fluorescence intensity is obtained; and the limit of detection, defined as three times of the standard deviation of background,[53, 54] was calculated to be 15 nM. These results indicate that CNPs-Hg^{2+} system can be applied as a fluorescence turn-on sensor for Cys detection in aqueous solutions with a reasonably high sensitivity.[55-57]

Remarkably, the sequential addition of constant amounts of Cys and Hg^{2+} to the aqueous solution of CNPs-Hg^{2+} gives rise to an alternative change of the system's PL intensity, as illustrated in Fig. 4d. These reversible fluorescence "ON-OFF" processes could be repeated for more than 10 times with the "ON"-state fluorescence intensity retention of over 85% of the initial fluorescence of CNPs. Even in the presence of 0.5 mM Hg^{2+}, the PL of CNPs is able to be recovered through addition of 1 mM Cys.

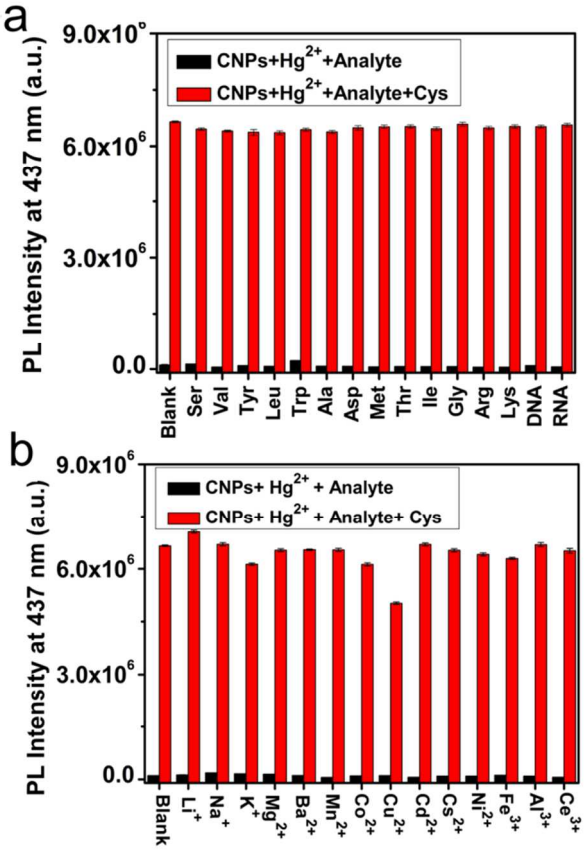

Fig. 5. (a) Selectivity of CNPs-Hg^{2+} system to Cys in the presence of amino acids or DNA, RNA in HEPES buffer solution (10 mM, pH 7.2). (b) Influence of impurity metal ions on the performance of CNPs-Hg^{2+} sensor. The black and red columns refer to the CNPs-Hg^{2+} mixture solution in the absence and presence of 20 μM Cys, respectively. Blank refers to free CNPs-Hg^{2+} mixture solution. The error bars represent standard deviations based on three independent measurements. The concentration of competing species was 20 μM.

The specificity of CNPs-Hg^{2+} sensor to mercapto thiol molecules

The complexity of intracellular systems presents great challenges to mercapto biomolecule detection. These are not only in the aspect of sensitivity but more importantly in selectivity because there are many types of amino acids, DNA and RNA in living systems. To verify the selectivity of CNPs-Hg^{2+} system to mercapto biomolecules, the PL response of CNPs-Hg^{2+} solution to other amino acids, RNA, and DNA was monitored and the results are presented in Fig. 5a. It is clear that only thiol-containing compounds (Cys, Hcy and GSH) result in a significant PL enhancement (Fig. S11). In contrast, other amino acids such as Ser, Val, Tyr, Leu, Trp, Ala, Asp, Met, Thr, Ile, Gly, Arg, and Lys as well as RNA and DNA do not induce any obvious changes of the system's PL properties (Fig. 5b, black columns). Notably, even in the presence of these species, the PL of CNPs-Hg^{2+} solution can be recovered by addition of Cys (Fig. 5a, red columns). These results clearly suggested that the CNPs-Hg^{2+} system has an excellent selectivity to biothiols. However, our experiments also revealed that, S^{2-} could also completely recover the PL of the CNPs-Hg^{2+}

solution due to its high affinity with Hg^{2+}. Moreover, addition of histidine increased the PL of CNPs-Hg^{2+} solution slightly, but did not affect the PL recovery. In contrast, excessive Ag^{+} had negligible influence on the PL of CNPs-Hg^{2+} solution but caused a reduced PL recovery efficiency, as illustrated in Fig. S12.

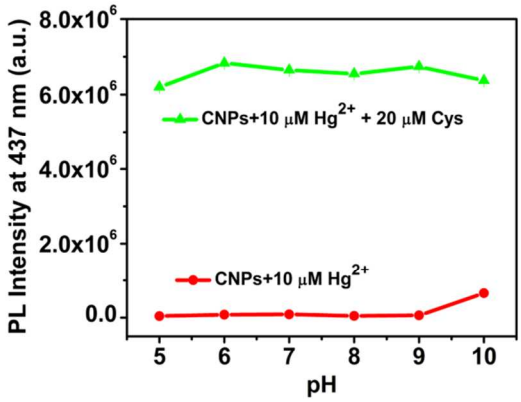

Fig. 6. Effect of pH on the PL intensity at 437 nm of CNPs-Hg^{2+} (red line) and CNPs-Hg^{2+}/Cys (green line) solutions at room temperature.

Influence of impurity metal ions on the performance of CNPs-Hg^{2+} sensor

It is important for a sensor to work in the interference of other parameters. As one test case, we studied the interference of other metal ions, including Li^{+}, Na^{+}, K^{+}, Mg^{2+}, Ba^{2+}, Mn^{2+}, Co^{2+}, Cu^{2+}, Cd^{2+}, Cs^{2+}, Ni^{2+}, Fe^{3+}, Al^{3+}, and Ce^{3+}, to the sensing performance of CNPs-Hg^{2+} in HEPES buffer solution (10 mM, pH 7.2). As illustrated in Fig. 5b (black columns), the PL intensities at 437 nm are relatively constant in the presence of all of the tested metal ions, probably due to the stronger affinity of Hg^{2+} with the amino and carboxylic groups on CNP surfaces as compared with the added metal ions. Furthermore, it is also observed that the PL of CNPs-Hg^{2+} solution can be greatly increased upon addition of Cys even in the presence of these interfering metal ions (Fig. 5b, red columns).

Influence of pH on the performance of CNPs-Hg^{2+} sensor

The effect of pH values on the PL stability of CNPs-Hg^{2+} system was also investigated. Fig. 6 shows the pH-dependent PL intensities at 437 nm of CNPs-Hg^{2+}, and CNPs-Hg^{2+}/Cys in aqueous solutions. It is found that the PL of CNPs-Hg^{2+} is constantly low within the pH range from 5 to 9 (red line) and, upon addition of Cys, the PL of CNPs-Hg^{2+} system massively enhances and maintain a relatively stable value (green line). These findings demonstrate the CNPs-Hg^{2+} system is very stable in the pH range of 5 to 9 which covers physiological condition. Hence, the excellent pH stability of the CNPs-Hg^{2+} system suggests its great potential for intercellular sensing and imaging.

In a recent work by Zhou *et al.*,[44] CNPs were prepared by pyrolysis of ethylenediamine-tetraacetic acid (EDTA) salts at 400 ^{o}C in flowing N_2. It was observed that the fluorescence quantum yield of CNPs decreases from 11.0% to 8.9% at 5 minutes after addition of Hg^{2+}, and the fluorescence intensity at 410 nm increases by ~30% upon addition of 2 eq Cys at pH 8.5. The relatively low quenching efficiency and its strong pH dependence may be due to the presence of only some hydroxyl and carboxylic surface groups on their CNPs synthesized at high temperature. In comparison, our CNPs are prepared under moderate conditions, and their surfaces are rich with amino, hydroxyl and carboxylic/carbonyl moiety functional groups. These groups, in particular amino group, serve as a key acceptor to Hg^{2+}, and thus the PL of our CNPs is completely quenched by Hg^{2+} and recovered by Cys in a wide pH range, enabling the CNPs-Hg^{2+} system to be an effective sensor for sensing mercapto biomolecules with high sensitivity and selectivity.

Detection and bioimaging of Cys in living cells

Once we demonstrate the CNPs-Hg^{2+} system has high sensitivity and specificity for the detection of mercapto thiols and can work with high performance at different pHs and along with the interference of various metal ions, the next step is to test whether our approach can be used for detection of biothiols in living systems. Before the test, it is essential to measure the cytotoxicity of the CNPs-Hg^{2+} system. This was performed with MTT assays and the results are in Fig. 7a. The viability of the A549 cells does not show obvious decrease in comparison that of the control group (without addition of CNPs-Hg^{2+} ions). Owing to the large amount of mercapto biomolecules in the cell, a concentration of Hg^{2+} (10 μM) under our experimental condition does not induce obvious cell death. Furthermore, a z-stack of confocal laser scanning microscopy images verifies that the CNPs can be uptaken into the cells, rather than just being adsorbed on the surfaces of cells (Fig. S13 and S14).[58, 59] Thus, the as-prepared CNPs-Hg^{2+} system can be considered to be low cytotoxicity and biocompatible for detection of biothiols in living cells.

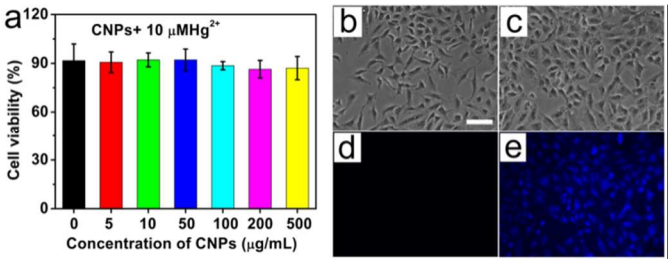

Fig. 7. (a) Cell viability values (%) estimated by MTT proliferation tests versus incubation concentrations of CNPs (0, 5, 10, 50, 100, 200, 500 μg/mL) in the presence of 10 μM Hg^{2+} at 37 ^{o}C for 24 h. Bright-field and fluorescence images of A549 cells incubated with CNPs-Hg^{2+} (b, d) and CNPs-Hg^{2+}/Cys (c, e). The scale bar is 40 μm.

The application of the CNPs-Hg^{2+} system for detecting mercapto biomolecules in living cells was demonstrated. Fig. 7b-e shows the bright field and fluorescence images of living A549 cells incubated with CNPs-Hg^{2+}, and CNPs-Hg^{2+}/Cys. As the cells were incubated with CNPs-Hg^{2+}, no obvious

fluorescence signal was observed (Fig. 8d). When these cells were further incubated with foreign addition of Cys, obvious strong blue fluorescence can be observed (Fig. 8e) due to the decomplexation of intracellular CNPs-Hg^{2+} to fluorescence CNPs by Cys uptake, demonstrating the potential of CNPs-Hg^{2+} system in thiol sensing in living cells.

Conclusions

In summary, water-soluble CNPs with strong blue emission were synthesized, and their fluorescence could be completely quenched by Hg^{2+}. Based on that, a highly selective and sensitive CNPs-Hg^{2+} fluorescence sensor for mercapto biomolecules was designed. The CNPs-Hg^{2+} system exhibits a rapid fluorescence turn on response to Cys with a detection limit of as low as 15 nM, and the sensor can be regenerated for recyclable use by subsequent addition of Hg^{2+}. After 10 recycles of use, the PL intensity of the system can still achieve as high as 85% of the original PL value of CNPs. Notably, This sensor is very specific to mercapto thiols and can work with high performance at different pHs and along with the interference of a variety of metal ions. With these superior advantages, the CNPs-Hg^{2+} system is capable of in vivo detection of biothiols.

Acknowledgements

This work was supported by Research Grants Council of the Hong Kong Special Administrative Region, China (Project No. CityU 102010) and National Natural Science Foundation of China (NSFC Grants 51372213 and 51172244).

Notes and references

[a] Center of Super-Diamond and Advanced Films (COSDAF), Department of Physics and Materials Science, City University of Hong Kong, Hong Kong SAR, P. R. China. Tel: +(852)-34427433, Fax: +(852)-34420538. E-mail: apwjzh@cityu.edu.hk

[b] Key Laboratory of Photochemical Conversion and Optoelectronic Materials, Technical Institute of Physics and Chemistry (TIPC), Chinese Academy of Sciences (CAS), Beijing, 100190, P. R. China. E-mail: wangpf@mail.ipc.ac.cn

Electronic Supplementary Information (ESI) available: details of spectra data. See DOI: 10.1039/b000000x/

1 J. D. Finkelstein and J. J. Martin, *Int. J. Biochem. Cell Biol.,* 2000, **32**, 385.
2 S. M. Deneke, *Curr. Top Cell Regul.,* 2000, **36**, 151.
3 X. G. Chen, Y. Zhou and X. J. Peng, J. Yoon, *Chem. Soc. Rev.,* 2010, **39**, 2120.
4 L. A. Herzenberg, S. C. De Rosa, J. G. Dubs, M. Roederer, M. T. Anderson, S. W. Ela, S. C. Deresinski and L. A. Herzenberg, *Proc. Natl. Acad. Sci. USA*, 1997, **94**, 1967.
5 S. Shahrokhian, *Anal. Chem.,* 2001, **73**, 5972.
6 R. Carmel and D. W. Jacobsen, *Homocysteine in Health and Disease*, Cambridge University Press: Cambridge, U.K. 2001.
7 D. M. Townsend, K. D. Tew and H. Tapiero, *Biomed. Pharmacother.,* 2003, **57**, 145.
8 P. Capitan, T. Malmezat, D. Breuillé and C. Obled, *J. Chromatogr. B: Biomed. Sci. Appl.* 1999, **732**, 127.
9 Y. Hiraku, M. Murata and S. Kawanishi, *Biochim. Biophys. Acta.,* 2002, **1570**, 47.
10 X. Guan, B. Hoffman, C. Dwivedi and D. P. Matthees, *J. Pharm. Biomed. Anal.,* 2003, **31**, 251.
11 W. Chen, Y. Zhao, T. Seefeldt and X. M. Guan, *J Pharm Biomed Anal.,* 2008, **48**, 1375.
12 C. Lodeiro, J. L. Capelo, J. C. Mejuto, E. Oliveira, H. M. Santos, B. Pedras and C. Nunez, *Chem. Soc. Rev.,* 2010, **39**, 2948.
13 J. S. Wu, W. M. Liu, J. C. Ge, H. Y. Zhang and P. F. Wang, *Chem. Soc. Rev.*, 2011, **40**, 3483.
14 M. H. Lan, J. S. Wu, W. M. Liu, W. J. Zhang, J. C. Ge, H. Y. Zhang, J. Y. Sun, W. W. Zhao and P. F. Wang, *J. Am. Chem. Soc.,* 2012, **134**, 6685.
15 M. H. Lan, W. M. Liu, J. C. Ge, J. S. Wu, H. J. Wang, W. J. Zhang, Y. F. Bi and P. F. Wang, *Chem. Commun.,* 2012, **48**, 6818.
16 M. H. Lan, W. M. Liu, Y. Wang, J. C. Ge, J. S. Wu, H. Y. Zhang, J. H. Chen, W. J. Zhang and P. F. Wang, *ACS Appl. Mater. Interfaces,* 2013, **5**, 2283.
17 W. H. Wang, J. O. Escobedo, C. M. Lawrence and R. M. Strongin, *J. Am. Chem. Soc.,* 2004, **126**, 3400.
18 H. Maeda, H. Matsuno, M. Ushida, K. Katayama, K. Saeki and N. Itoh, *Angew. Chem., Int. Ed.,* 2005, **44**, 2922.
19 W. Y. Lin, L. L. Long, L. Yuan, Z. M. Cao, B. B. Chen and W. Tan, *Org. Lett.,* 2008, **10**, 5577.
20 S. Huang, Q. Xiao, R. Li, H. L. Guan, J. Liu, X. R. Liu, Z. K. He and Y. Liu, *Anal. Chim. Acta.,* 2009, **645**, 73.
21 J. S. Wu, R. L. Sheng, W. M. Liu, P. F. Wang, J. J. Ma, H. Y. Zhang and X. Q. Zhuang, *Inorg. Chem.,* 2011, **50**, 6543.
22 A. Y. Cho and K. H. Choi, *Chem. Lett.,* 2012, **41**, 1611.
23 X. Y. Xu, R. Ray, Y. L. Gu, H. J. Ploehn, L. Gearheart, K. Raker and W. A. Scrivens, *J. Am. Chem. Soc.,* 2004, **126**, 12736.
24 S. N. Baker and G. A. Baker, *Angew. Chem. Int. Ed.,* 2010, **49**, 6726.
25 S. N. Qu, X. Y. Wang, Q. P. Lu, X. Y. Liu and L. J. Wang, *Angew. Chem. Int. Ed.,* 2012, **51**, 12215.
26 C. Y. Wu, C. Wang, T. Han, X. J. Zhou, S. W. Guo and J. Y. Zhang, *Adv. Healthcare Mater.,* 2013, **2**, 1613.
27 R. Q. Ye, C. S. Xiang, J. Lin, Z. W. Peng, K. W. Huang, Z. Yan, N. P. Cook, E. L. G. Samuel, C. C. Hwang, G. D. Ruan, G. Ceriotti, A. R. O. Raji, A. A. Marti and J. M. Tour, *Nat. Commun.,* 2013, **4**, 2943.
28 S. Liu, J. Q. Tian, L. Wang, Y. W. Zhang, X. Y. Qin, Y. L. Luo, A. M. Asiri, A. O. Al-Youbi, X. P. Sun, *Adv. Mater.*, 2012, **24**, 2037.
29 X. Y. Qin, W. B. Lu, A. M. Asiri, A. O. Al-Youbi, X. P. Sun, *Catal. Sci. & Technol.*, 2013, **3**, 1027.
30 X. Y. Qin, S. Liu, W. B. Lu, H. Y. Li, G. H. Chang, Y. W. Zhang, J. Q. Tian, Y. L. Luo, A. M. Asiri, A. O. Al-Youbi, X. P. Sun, *Catal. Sci. & Technol.*, 2012, **2**, 711.
31 S. Liu, J. Q. Tian, L. Wang, Y. L. Luo, X. P. Sun, *RSC Adv.*, 2012, **2**, 411.
32 S. Liu, L. Wang, J. Q. Tian, J. F. Zhai, Y. L. Luo, W. B. Lu, X. P. Sun, *RSC Adv.*, 2011, **1**, 951.

33 S. Liu, J. Q. Tian, L. Wang, Y. L. Luo, J. F. Zhai, X. P. Sun, *J. Mater. Chem.*, 2011, **21**, 11726.
34 X. Y. Qin, W. B. Lu, A. M. Asiri, A. O. Al-Youbi, X. P. Sun, *Sens. Actuator B,* 2013, **184**, 156.
35 X. Y. Qin, A. M. Asiri, K. A. Alamry, A. O. Al-Youbi, X. P. Sun, *Electrochim. Acta.*, 2013, **95**, 260.
36 W. B. Lu, X. Y. Qin, A. M. Asiri, A. O. Al-Youbi, X. P. Sun, *J. Nanopart. Res.*, 2013, **15**, 1344.
37 X. Y. Qin, W. B. Lu, G. H. Chang, Y. L. Luo, A. M. Asiri, A. O. Al-Youbi, X. P. Sun, *Gold Bulletin*, 2012, **45**, 61.
38 W. B. Lu, X. Y. Qin, S. Liu, G. H. Chang, Y. W. Zhang, Y. L. Luo, A. M. Asiri, A. O. Al-Youbi and X. P. Sun, *Anal. Chem.,* 2012, **84**, 5351.
39 A. W. Zhu, Q. Qu, X. L. Shao, B. Kong and Y. Tian, *Angew. Chem. Int. Ed.,* 2012, **51**, 7185.
40 Y. H. Wang, L. Bao, Z. H. Liu and D. W. Pang, *Anal. Chem.,* 2011, **83**, 8130.
41 S. Maiti, K. Das and P. K. Das, *Chem. Commun.,* 2013, **49**, 8851.
42 X. Y. Ouyang, J. H. Liu, J. S. Li and R. H. Yang, *Chem. Commun.,* 2012, **48**, 88.
43 C. M. Yu, X. Z. Li, F. Zeng, F. Y. Zheng and S. Z. Wu, *Chem. Commun.,* 2013, **49**, 403.
44 L. Zhou, Y. H. Lin, Z. Z. Huang, J. S. Ren and X. G. Qu, *Chem. Commun.,* 2012, **48**, 1147.
45 Y. P. Shi, Y. Pan, H. Zhang, Z. M. Zhang, M. J. Li, C. Q. Yi and M. S. Yang, *Biosens. Bioelectron.,* 2014, **56**, 39.
46 H. Peng and J. T. Sejdic, *Chem. Mater.,* 2009, **21**, 5563.
47 S. J. Zhu, Q. N. Meng, L. Wang, J. H. Zhang, Y. B. Song, H. Jin, K, Zhang, H. C. Sun, H. Y. Wang and B. Yang, *Angew. Chem. Int. Ed.,* 2013, **52**, 3953.
48 Z. S. Qian, J. J. Ma, X. Y. Shan, H. Feng, L. X. Shao and J. R. Chen, *Chem. Eur. J.,* 2014, **20**, 2254.
49 Y. Q. Zhang, D. K. Ma, Y. Zhuang, X. Zhang, W. Chen, L. L. Hong, Q. X. Yan, K. Yu and S. M. Huang, *J. Mater. Chem.,* 2012, **22**, 16714.
50 Z. L. Wu, P. Zhang, M. X. Gao, C. F. Liu, W. Wang, F. Leng and C. Z. Huang, *J. Mater. Chem. B,* 2013, **1**, 2868.
51 B. Y. Han, J. P. Yuan and E. K. Wang, *Anal. Chem.,* 2009, **81**, 5569.
52 F. Pu, Z. Z. Huang, J. S. Ren and X. G. Qu, *Anal. Chem.,* 2010, **82**, 8211.
53 J. Zheng, J. S. Li, X. X. Gao, J. Y. Jin, K. M. Wang, W. H. Tan and R. H. Yang, *Anal. Chem.,* 2010, **82**, 3914.
54 C. Kar, M. D. Adhikari, A. Ramesh and G. Das, *Inorg. Chem.,* 2013, **52**, 743.
55 M. H. Lan, J. S. Wu, W. M. Liu, H. Y. Zhang, W. J. Zhang, X. Q. Zhuang and P. F. Wang, *Sens. Actuators, B-Chem.,* 2011, **156**, 332.
56 B. Liu, J. F. Wang, G. Zhang, R. K. Bai and Y. Pang, *ACS Appl. Mater. Interfaces,* 2014, **6**, 4402.
57 H. M. Lv, X. F. Yang, Y. G. Zhong, Y. Guo, Z. Li and H. Li, *Anal. Chem.,* 2014, **86**, 1800.
58 S. H. Hu, Y. W. Chen, W. T. Hung, I. W. Chen and S. Y. Chen, *Adv. Mater.,* 2012, **24**, 1748.
59 S. H. Hu, R. H. Fang, Y. W. Chen, B. J. Liao and S. Y. Chen, *Adv. Funct. Mater.,* 2014, **24**, 4144.

TOC figure

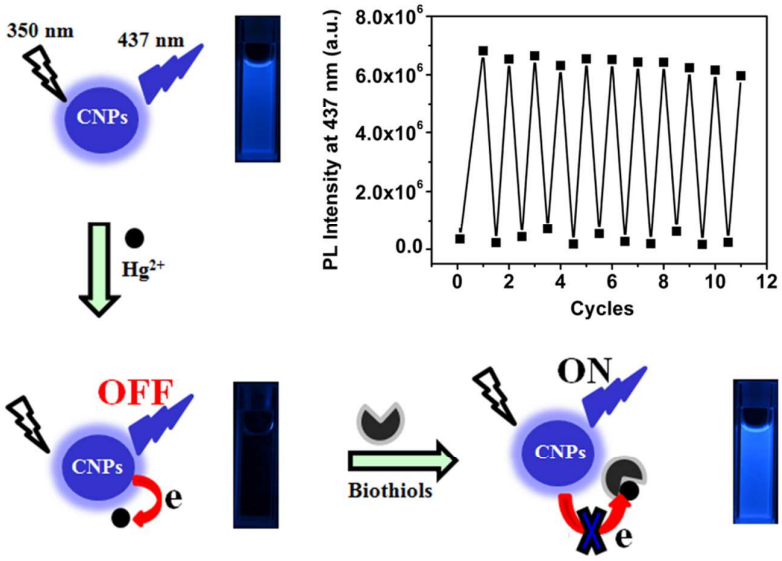

Hg^{2+} quenched CNPs (CNPs-Hg^{2+}) was reported as a highly sensitive and selective reversible probe for the detection of mercapto biomolecules in aqueous solution and in living cells.